Spin-determination of the Randall-Sundrum graviton resonance at the LHC

A. A. Pankov[a*] and A. V. Tsytrinov[a†]

[a] *The Abdus Salam ICTP Affiliated Centre, Technical University of Gomel*
October Ave. 48, Gomel 246746 Belarus

Abstract

The determination of the spin of the intermediate quantum states exchanged in the various non-standard interactions is a relevant aspect in the identification of the corresponding scenarios. We discuss the *identification* reach at LHC on the spin-2 of the lowest-lying Randall-Sundrum graviton resonance, predicted by gravity with one warped extra dimension, against spin-1 (Z') and spin-0 (sneutrino in $\not{R}_p$ SUSY) non-standard exchanges with the same mass and producing the same number of events in the cross section. We focus on the angular distributions of leptons produced in the Drell-Yan process at the LHC, in particular we use as basic observable the central-edge asymmetry $A_{\rm CE}$. We find that the 95% C.L. *identification* reach on the spin-2 of the RS graviton resonance is up to a resonance mass scale of the order of 1.6 TeV in the case of weak coupling between graviton excitations and SM particles ($k/\bar{M}_{Pl} = 0.01$) and 3.2 TeV for larger coupling constant ($k/\bar{M}_{Pl} = 0.1$) for a time-integrated LHC luminosity of $100\,\mathrm{fb}^{-1}$.

1 Introduction

A general feature of the different New Physics (NP) scenarios beyond the Standard Model (SM) is the prediction of heavy new particles or "resonances", that can be either produced or exchanged in reactions studied at high energy colliders. Such non-standard objects are expected to be in the TeV mass range, and could be revealed directly as peaks in the energy dependence of the measured cross sections. For any model one can determine the corresponding *discovery* reach by determining the upper limit of the mass range where the resonance signal can be detected above the SM cross section to a given confidence level.

On the other hand, once a peak in the cross section is observed, further analysis is needed to distinguish the underlying non-standard dynamics against the other scenarios that potentially may cause a similar effect. In this regard, the expected *identification* reach is defined as the upper limit of the mass range where the model could be identified as the source of the peak or, equivalently, the other competitor models can be excluded for all values of their parameters. The determination of the spin of the resonance represents therefore an important selection among different classes of non-standard interactions [1].

Here, we consider the discrimination reach on the lowest-lying spin-2 Randall–Sundrum (RS) graviton resonance [2], that could be obtained from measurements of the Drell–Yan (DY) lepton-pair production processes at the LHC:

$$p + p \to l^+ l^- + X. \tag{1}$$

where $l = e, \mu$.

*e-mail: pankov@ictp.it
†e-mail: tsytrin@gstu.gomel.by

The determination of the spin-2 of the lowest-lying RS graviton resonance exchange against the spin-1 hypothesis in the context of experiments at LHC has recently been discussed, e.g., in Refs. [3, 4, 5, 6, 7, 6, 8]. An experimental search for spin-2, spin-1 and spin-0 new particles decaying to DY dilepton pairs has recently been performed at the Fermilab Tevatron $p\bar{p}$ collider [9].

We would like to complement those analyses and assess the extent to which the domain in the RS parameters allowed by the discovery reach on the resonance is reduced by the request of simultaneous exclusion of *both* the hypotheses of spin-1 and spin-0 exchanges with the same mass, and mimicking the same peak in the dilepton invariant mass distribution (same number of events).

As is well known, the main tool to differentiate among the spin exchanges in the process (1) uses the different, and characteristic, dependencies on the angle $\theta_{\rm cm}$ between the incident quark or gluon and the final lepton in the dilepton center-of-mass frame. We shall base our discussion on the integrated center-edge asymmetry $A_{\rm CE}$, that has the property of directly disentangling the spin-2 from vector interactions as illustrated in Refs. [10, 11]. This method represents an alternative to the use of the differential distributions $\mathrm{d}N/\mathrm{d}\cos\theta_{\rm cm}$, where N represents the number of events.

As an example of spin-0 contribution to the process (1), we can consider the sneutrino exchange envisaged by supersymmetric theories with R-parity breaking ($\not{R}_p$) [12, 13]. In $\not{R}_p$ it is possible that some sparticles can be produced as s-channel resonances, thus appearing as peaks in the dilepton invariant mass distribution, if kinematically allowed.

Examples of competitor spin-1 mediated interactions, that can contribute to process (1) and show up as peaks in the cross section are, besides the SM γ and Z, the heavy Z' exchanges [14], and we will refer to those models for the comparison with the RS resonance exchange.

2 RS graviton resonance production at the LHC

In the RS scenario TeV-scale, spin-2, narrow graviton resonances are predicted. The model depends on two independent parameters, that can be chosen as the dimensionless ratio $c = k/\bar{M}_{Pl}$, with k the 5-dimensional scalar curvature and $\bar{M}_{Pl}$ the reduced 4-dimensional Planck scale ($\bar{M}_{Pl} = M_{Pl}/\sqrt{8\pi}$), and m_1, the mass of the lowest-lying graviton resonance. The masses of the higher excitations $G^{(n)}$ are given by $m_n = m_1\, x_n/x_1$, where x_n are roots of the Bessel function $J_1(x_n) = 0$ ($x_1 = 3.8317$, $x_2 = 7.0156$, $x_3 = 10.1735$,..), and are therefore unevenly spaced. The mass pattern may therefore be distinctive of the model, if higher excitations in addition to the ground state would be discovered. A correlated parameter is represented by the physical scale on the TeV brane $\Lambda_\pi = m_1/(c\, x_1)$, whose inverse controls the strength of the graviton resonance coupling to standard matter. The (theoretically) natural ranges for these parameters are $0.01 \leq c \leq 0.1$ and $\Lambda_\pi < 10\,\mathrm{TeV}$ [15]. Current discovery limits at 95% C.L. from the Fermilab Tevatron collider are for the first graviton mass: 300 GeV for $c = 0.01$ and 900 GeV for $c = 0.1$ [16].

In the SM, lepton pairs at hadron colliders can be produced at tree level via the following parton-level processes:

$$q\bar{q} \to \gamma, Z \to l^+l^-. \tag{2}$$

The first massive graviton mode $G^{(1)}$ of the RS model, in the sequel denoted simply as G (and the mass $m_1 \equiv M_G$), can be produced via quark–antiquark annihilation as well as gluon–gluon fusion,

$$q\bar{q} \to G \to l^+l^- \qquad \text{and} \qquad gg \to G \to l^+l^-, \tag{3}$$

and can be observed as a peak in the dilepton invariant mass distribution. The inclusive differential cross section for G production and subsequent decay into lepton pairs at the LHC

can be expressed as the sum:

$$\frac{\mathrm{d}\sigma}{\mathrm{d}M\,\mathrm{d}y\,\mathrm{d}z} = \frac{\mathrm{d}\sigma_{q\bar{q}}}{\mathrm{d}M\,\mathrm{d}y\,\mathrm{d}z} + \frac{\mathrm{d}\sigma_{gg}}{\mathrm{d}M\,\mathrm{d}y\,\mathrm{d}z}, \tag{4}$$

where M and y are invariant mass and rapidity of the lepton pairs, respectively, and $z = \cos\theta_{\rm cm}$ with $\theta_{\rm cm}$ the lepton-proton angle in the dilepton center-of-mass frame. Explicitly:

$$\begin{aligned}\frac{\mathrm{d}\sigma_{q\bar{q}}}{\mathrm{d}M\,\mathrm{d}y\,\mathrm{d}z} = K\frac{2M}{s}\sum_q \Bigg\{ &[f_{q|P_1}(\xi_1,M) f_{\bar{q}|P_2}(\xi_2,M) + f_{\bar{q}|P_1}(\xi_1,M) f_{q|P_2}(\xi_2,M)]\frac{\mathrm{d}\hat{\sigma}^{\rm even}_{q\bar{q}}}{\mathrm{d}z} \\ &+[f_{q|P_1}(\xi_1,M) f_{\bar{q}|P_2}(\xi_2,M) - f_{\bar{q}|P_1}(\xi_1,M) f_{q|P_2}(\xi_2,M)]\frac{\mathrm{d}\hat{\sigma}^{\rm odd}_{q\bar{q}}}{\mathrm{d}z}\Bigg\}, \\ \frac{\mathrm{d}\sigma_{gg}}{\mathrm{d}M\,\mathrm{d}y\,\mathrm{d}z} = K\frac{2M}{s}\, &f_{g|P_1}(\xi_1,M) f_{g|P_2}(\xi_2,M)\frac{\mathrm{d}\hat{\sigma}_{gg}}{\mathrm{d}z}. \end{aligned} \tag{5}$$

Here, $\mathrm{d}\hat{\sigma}^{\rm even}_{q\bar{q}}/\mathrm{d}z$ and $\mathrm{d}\hat{\sigma}^{\rm odd}_{q\bar{q}}/\mathrm{d}z$ are the even and odd parts (under $z \leftrightarrow -z$) of the partonic differential cross section $\mathrm{d}\hat{\sigma}_{q\bar{q}}/\mathrm{d}z$. Furthermore, the K-factor accounts for higher order QCD corrections (see, for instance Ref. [17]). Finally, $f_{j|P_i}(\xi_i, M)$ are parton distribution functions in the protons P_1 and P_2, and ξ_i are the parton fractional momenta:

$$\xi_1 = \frac{M}{\sqrt{s}}\, e^{y}, \qquad \xi_2 = \frac{M}{\sqrt{s}}\, e^{-y}. \tag{6}$$

In deriving Eq. (5), the relations $\mathrm{d}\xi_1\,\mathrm{d}\xi_2 = (2M/s)\mathrm{d}M\mathrm{d}y$ and $M^2 = \xi_1\xi_2 s$ have been used, with s the pp C.M. energy squared. The minus sign in the odd term in that equation allows us to interpret the angle $\theta_{\rm cm}$ in the parton cross section as being relative to the quark or gluon momentum (rather than the proton momentum P_1).

The lepton differential angular distribution, for dilepton invariant mass M in an interval of size ΔM around the (narrow) resonance peak M_R, is defined by

$$\frac{\mathrm{d}\sigma}{\mathrm{d}z} = \int_{M_R-\Delta M/2}^{M_R+\Delta M/2} \mathrm{d}M \int_{-Y}^{Y} \frac{\mathrm{d}\sigma}{\mathrm{d}M\,\mathrm{d}y\,\mathrm{d}z}\,\mathrm{d}y, \tag{7}$$

with $Y = \log(\sqrt{s}/M)$.

The cross section for the narrow state production and subsequent decay into a DY pair, $pp \to R \to l^+l^-$, is given by:

$$\sigma(R_{ll}) \equiv \sigma(pp\to R)\cdot \mathrm{BR}(R\to l^+l^-) = \int_{-z_{\rm cut}}^{z_{\rm cut}} \mathrm{d}z \int_{M_R-\Delta M/2}^{M_R+\Delta M/2} \mathrm{d}M \int_{-Y}^{Y} \mathrm{d}y \frac{\mathrm{d}\sigma}{\mathrm{d}M\,\mathrm{d}y\,\mathrm{d}z}. \tag{8}$$

Actually, if angular cuts are imposed by detector acceptance, $|z| \le z_{\rm cut}$, then Y in Eqs. (7) and (8) must be replaced by some maximum value, $y_{\rm max} = y_{\rm max}(z)$.

One may notice that only terms in the partonic cross sections which are even in z contribute to the right-hand side of Eq. (7), because in the case of the proton-proton collider odd terms do not contribute after the integration over the rapidity y. This holds true for the SM γ-Z interference term, as well as for SM-G interference, with the SM partonic cross section being pure $q\bar{q}$-initiated at the considered order. Although such interference terms may appreciably contribute to the doubly-differential cross section $\mathrm{d}\sigma/\mathrm{d}M\mathrm{d}z$, their contribution to the integral over M needed in Eqs. (7) and (8), symmetrical around the graviton resonance mass M_R, is negligibly small for $M_Z \ll M_R$ and small resonance width (an approximation that will be assumed in the sequel), and negligible M-dependence of the overlap integral within the ΔM bin. This fact is pointed out for the case of Z's in, e.g., Refs. [8, 17], but also holds for the graviton resonance case. Thus, in Eqs. (7) and (8), we can just retain the SM and the G pole contributions.

Keeping z-symmetric terms only, the partonic cross sections relevant to the analysis presented below read [18, 19] (we follow the notation of [10]):

$$\left.\frac{\mathrm{d}\hat{\sigma}^G_{q\bar{q}}}{\mathrm{d}z}+\frac{\mathrm{d}\hat{\sigma}^G_{gg}}{\mathrm{d}z}\right|_{z\ \mathrm{even}}=\frac{\kappa^4 M^2}{640\pi^2}\left[\Delta_{q\bar{q}}(z)+\Delta_{gg}(z)\right]|\chi_G|^2, \tag{9}$$

$$\left.\frac{\mathrm{d}\hat{\sigma}^{\mathrm{SM}}_{q\bar{q}}}{\mathrm{d}z}\right|_{z\ \mathrm{even}}=\frac{\pi\alpha^2_{\mathrm{em}}}{6M^2}\left[S_q\,(1+z^2)\right]. \tag{10}$$

In Eq. (9), χ_G represents the graviton G propagator, with M_G and Γ_G the mass and total width, respectively:

$$\chi_G=\frac{M^2}{M^2-M_G^2+i\,M_G\Gamma_G}, \tag{11}$$

and, for the first massive mode, κ is given by [4, 20]

$$\kappa=\sqrt{2}\,\frac{x_1}{M_G}\,c. \tag{12}$$

The total width can be written as $\Gamma_G=\rho\,x_1^2\,c^2\,M_G$, where ρ is a constant depending on the number of open decay channels. Assuming the graviton decays only to the SM particles, and with partial widths explicitly given in Refs. [4, 18, 20], one finds $\Gamma_G=1.43\,c^2\,M_G$. With $c\leq 0.1$ in the theoretically "natural" range, this value allows to use for the graviton resonance propagator the narrow-width approximation,

$$|\chi_G|^2\to\delta(M-M_G)\,\frac{\pi M_G^2}{2\,\Gamma_G}. \tag{13}$$

The leading order angular dependencies in Eq. (9) are given by

$$\Delta_{q\bar{q}}(z)=\frac{\pi}{8N_C}\,\frac{5}{8}\,(1-3z^2+4z^4),\qquad \Delta_{gg}(z)=\frac{\pi}{2(N_C^2-1)}\,\frac{5}{8}\,(1-z^4), \tag{14}$$

where N_C is the number of quark colors.

For the SM partonic cross section of Eq. (10) one has, neglecting fermion masses:

$$S_q\equiv Q_q^2Q_e^2+2Q_qQ_ev_qv_e\,\mathrm{Re}\,\chi_Z+(v_q^2+a_q^2)(v_e^2+a_e^2)\,|\chi_Z|^2, \tag{15}$$

where, for fermion f, $a_f=T_{3f}$, $v_f=T_{3f}-2Q_f\sin^2\theta_W$, and the Z propagator in the approximation $M\gg M_Z$ is represented by

$$\chi_Z(M)\approx\frac{1}{\sin^2(2\theta_W)}\,\frac{M^2}{M^2-M_Z^2}. \tag{16}$$

In the experimental discovery of a narrow resonance the observed width is determined by the dilepton invariant mass resolution, that we may associate to the size of the bin ΔM introduced above. Regarding the bin size, it depends on the energy resolution. For example, for the ATLAS detector, the bin size ΔM at invariant dilepton mass M measured in TeV units, can be parameterized as [21]:

$$\Delta M=24\,(0.625M+M^2+0.0056)^{1/2}\ \mathrm{GeV}. \tag{17}$$

Similar results, comparable to about 10%, hold for the CMS detector [22]. Throughout the paper we will use Eq. (17) for the bin size.

At the LHC, with integrated luminosity $\mathcal{L}_{\mathrm{int}}=100\ \mathrm{fb}^{-1}$, the number of signal (resonant) events can be computed by using $N_S=\sigma(R_{ll})\,\epsilon_l\,\mathcal{L}_{\mathrm{int}}$ and the background events are defined as $N_B=N_{SM}$ (background integrated over the bin). Here, ϵ_l is the experimental reconstruction

efficiency, taken to be 0.9 both for electrons and muons. To compute cross sections we use the CTEQ6 parton distributions [23]. We impose angular cuts relevant to the LHC detectors. The lepton pseudorapidity cut is $|\eta| < \eta_{\rm cut} = 2.5$ for both leptons (this leads to a boost-dependent cut on z [10]), and in addition to the angular cuts, we impose on each lepton a transverse momentum cut $p_\perp > p_\perp^{\rm cut} = 20$ GeV. Analogous to previous references, in the analysis given here, we have adopted the criterion for the discovery limit that $5\sqrt{N_B}$ events or 10 events, whichever is larger, constitutes a signal.

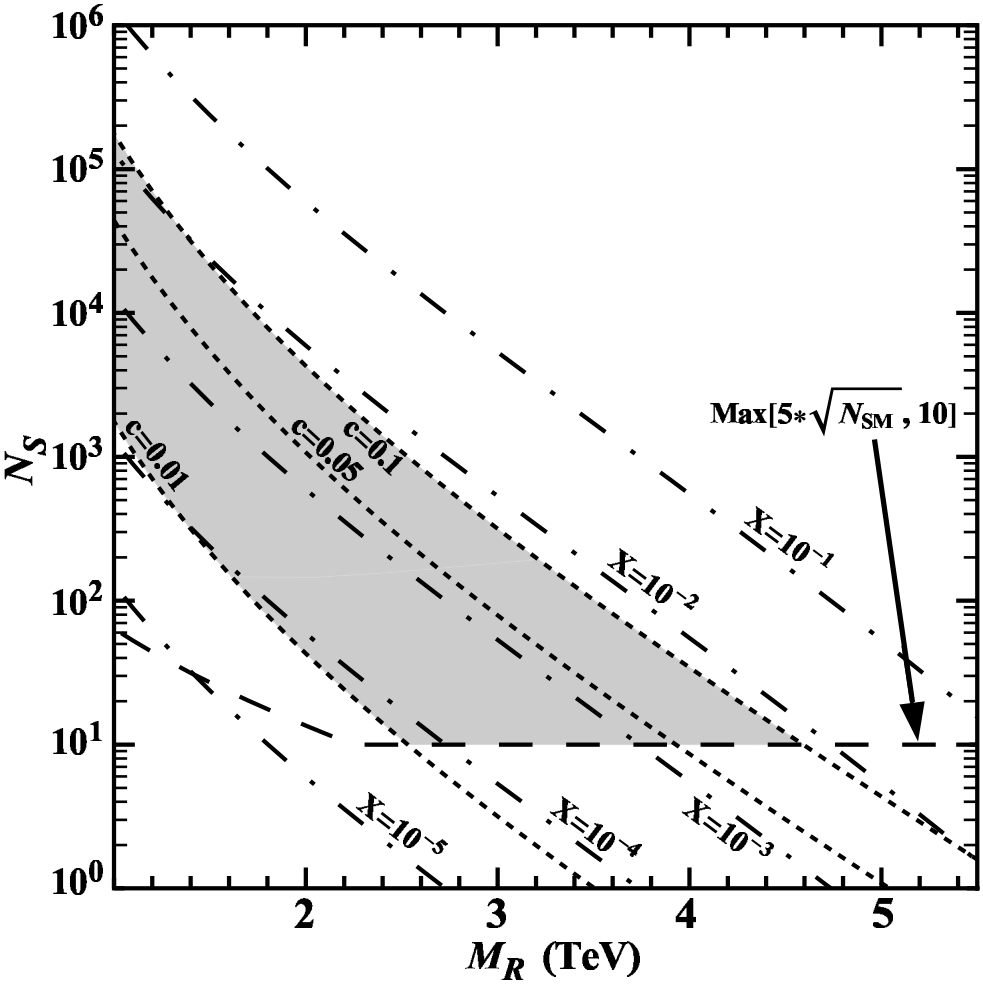

Figure 1: Expected number of resonance (signal) events N_S vs. M_R ($R = G, \tilde{\nu}_\tau$) at $\mathcal{L}_{\rm int} = 100$ fb^{-1} for graviton and sneutrino resonant production with values of c= 0.01, 0.05, 0.1 (short dashed curves) and X ranging from 10^{-5} to 10^{-1} in steps of 10 (dash-dotted curves) and the minimum number of signal events (dashed curve) needed to detect the resonance above the background in the process $pp \to l^+l^- + X$ ($l = e, \mu$). Shaded area corresponds to potential overlap of graviton signature space with that for sneutrino resonant production.

Fig. 1 shows the expected number of resonant (signal) events N_S *vs.* resonance mass M_R ($R = G$) at $\mathcal{L}_{\rm int} = 100$ fb^{-1} for graviton production with values of c= 0.01, 0.05, 0.1 (dashed curves), and the minimum number of signal events needed to detect it above the background. With the assumption of efficiencies as stated above one finds that, with 100 fb^{-1} of integrated luminosity, one can explore a massive graviton up to a mass of about 2.5 TeV with $c = 0.01$ (5σ level), and this limit can be pushed to ≈ 4.5 TeV with $c = 0.1$, consistent with the results of [15]. We shall refer to a region in the space spanned by resonance mass and number of events, that can be populated by a certain model, as the "signature space" of that model.

3 Signature spaces of RS G, sneutrino in $\not{R}_p$ and Z'

Models based on $\not{R}_p$ SUSY can mimic the RS graviton in a certain part of the parameter space as far as the mass and narrowness of the resonance is concerned. At tree-level, the relevant parton process for DY lepton-pair production is in R-parity breaking given by spin-0 sneutrino ($\tilde{\nu}$) formation from quark-antiquark annihilation and subsequent leptonic decay:

$$q\bar{q} \to \gamma, Z, \tilde{\nu} \to l^+ l^-. \tag{18}$$

The corresponding partonic cross section is given by [12]

$$\frac{\mathrm{d}\hat{\sigma}_{q\bar{q}}}{\mathrm{d}z} = \frac{\mathrm{d}\hat{\sigma}^{\mathrm{SM}}_{q\bar{q}}}{\mathrm{d}z} + \frac{\mathrm{d}\hat{\sigma}^{\tilde{\nu}}_{q\bar{q}}}{\mathrm{d}z}, \tag{19}$$

where the pure resonant term reads

$$\frac{\mathrm{d}\hat{\sigma}^{\tilde{\nu}}_{q\bar{q}}}{\mathrm{d}z} = \frac{1}{3}\,\frac{\pi\alpha^2_{\mathrm{em}}}{4\,M^2}\left(\frac{\lambda\lambda'}{e^2}\right)^2 |\chi_{\tilde{\nu}}|^2\,\delta_{qd}. \tag{20}$$

Here, the propagator of the sneutrino $\chi_{\tilde{\nu}}$ is represented by

$$\chi_{\tilde{\nu}} = \frac{M^2}{M^2 - M^2_{\tilde{\nu}} + i\,M_{\tilde{\nu}}\Gamma_{\tilde{\nu}}}, \tag{21}$$

$M_{\tilde{\nu}}$ ($\Gamma_{\tilde{\nu}}$) is the mass (total decay width) of the sneutrino, λ' and λ are the relevant R-parity-violating couplings of $d\bar{d}$ and l^+l^- to the sneutrino, respectively.

In the narrow width approximation the $\tilde{\nu}$-exchange cross section (20) can be written as:

$$\frac{\mathrm{d}\hat{\sigma}^{\tilde{\nu}}_{q\bar{q}}}{\mathrm{d}z} \approx \frac{\pi}{24}\,\frac{X}{M_{\tilde{\nu}}}\,\delta(M - M_{\tilde{\nu}})\,\delta_{qd}, \tag{22}$$

where

$$X = (\lambda')^2 B_l. \tag{23}$$

Here B_l is the sneutrino leptonic branching ratio and λ' the relevant coupling to the $d\bar{d}$ quarks.

Quantitatively, the current constraints on X are rather loose. The number of signal events as a function of the spin-0 mass for the case of sneutrino production with values of X ranging from 10^{-5} to 10^{-1} [13] in steps of 10 (dash-dotted curves), are given in Fig. 1. From Fig. 1 one can easily obtain the discovery reach on sneutrino parameters (5σ level).

In Fig. 1, the shaded area indicates the overlap of the LHC-discovery parameter space for the $\not{R}_p$ scenario *via* $\sigma(pp \to \tilde{\nu} \to l^+l^-)$ and that of the lowest RS graviton scenario *via* $\sigma(pp \to G \to l^+l^-)$. The figure indicates that, as far as the total production cross section of DY dilepton pairs is concerned, there exists a significantly extended domain in the $(M_{\tilde{\nu}}, X)$ plane where sneutrino $\tilde{\nu}$ production can mimic RS graviton G formation in its theoretically "natural" domain (M_G, c): in these respective domains, the two scenarios can lead to the same number of events under the resonance peak, $N_S(G \to l^+l^-) = N_S(\tilde{\nu} \to l^+l^-)$. In other words, the two models are indistinguishable in the overlapping domains of their parameter spaces, indicated by the shaded area in Fig. 1. Clearly, outside the "common" shaded area, the two scenarios might be differentiated by means of event rates. For the identification, the two models must be discriminated in the "confusion" region in Fig. 1, this can be done by the spin determination of the RS resonance.

Turning now to spin-1 resonance exchange, the differential cross section for the relevant partonic process $q\bar{q} \to \gamma, Z, Z' \to l^+l^-$ reads at leading order

$$\frac{\mathrm{d}\hat{\sigma}_{q\bar{q}}}{\mathrm{d}z} = \frac{\mathrm{d}\hat{\sigma}^{\mathrm{SM}}_{q\bar{q}}}{\mathrm{d}z} + \frac{\mathrm{d}\hat{\sigma}^{Z'}_{q\bar{q}}}{\mathrm{d}z}, \tag{24}$$

with

$$\left.\frac{\mathrm{d}\hat{\sigma}^{Z'}_{q\bar{q}}}{\mathrm{d}z}\right|_{z-\mathrm{even}} = \frac{\pi\alpha^2_{\mathrm{em}}}{6M^2}\,[S^{Z'}_q\,(1+z^2)], \tag{25}$$

and, neglecting fermion masses:

$$S^{Z'}_q \equiv (v'^2_q + a'^2_q)(v'^2_e + a'^2_e)\,|\chi_{Z'}|^2. \tag{26}$$

Here, we have introduced the Z' vector and axial-vector couplings to SM fermions, and the Z' propagator $\chi_{Z'}$ is represented by

$$\chi_{Z'} = \frac{M^2}{M^2 - M^2_{Z'} + i\,M_{Z'}\Gamma_{Z'}}. \tag{27}$$

According to previous arguments, in the sequel we neglect $(\gamma, Z) - Z'$ interference terms in the cross section. Moreover, effects from a potential $Z - Z'$ mixing are also disregarded.

In addition to a generic spin-1 exchange, we will consider the discrimination reach on the spin-2 lowest RS resonance from the, rather popular and physically motivated, Z' scenarios where the couplings in Eq. (26) are constrained to have fixed values. One such model is the so-called sequential model (SSM), where the Z' couplings to fermions are the same as those of the SM Z.

Furthermore, we will consider: (i) the three possible $U(1)\,Z'$ scenarios originating from the exceptional group E_6 breaking; and (ii) the Z' predicted by a left-right symmetric model that can originate from an $SO(10)$ GUT. While detailed descriptions of these models can be found, e. g., in Ref. [14], we just recall that the three heavy neutral gauge bosons are denoted by Z'_χ, Z'_ψ, Z'_η and Z'_{LR}, respectively.

The number of Z' signal events as a function of resonance mass for the representative models and LHC luminosity of 100 fb^{-1}, are given in Fig. 2. From this figure, one can easily obtain the 5σ level discovery reaches on the corresponding Z' masses.

In these cases, the Z' signature spaces reduce to lines, and Fig. 2 shows that, at the assumed LHC luminosity, the lowest, RS spin-2, resonance can be discriminated against the ALR and SSM spin-1 Z' scenarios already at the level of event rates in a large range of $M_{Z'}$ values, with no need for further analyses based on angular distributions. Only the E_6 and LR Z' models possess a "confusion region" with the RS resonance G, concentrated near the upper border of the graviton allowed signature domain.

4 Angular analysis and identification of the spin-2 of the RS graviton

The CDF collaboration has recently attempted angular distribution analyses using the cumulative DY data at the $p\bar{p}$ Tevatron collider, their results are reported in Ref. [9]. The LHC promises tests of the spin hypotheses with significantly higher sensitivity, due to the definitely higher statistics allowed by the foreseen larger energy and luminosity.

Using Eq. (7), one can derive the angular distributions determined by spin-2 RS graviton resonance, spin-1 V and spin-0 S, respectively. These distributions can be conveniently written in a self-explanatory way as [G denotes the spin-2 resonance, while V and S denote the spin-1 and spin-0 cases, respectively]:

$$\frac{\mathrm{d}\sigma(G_{ll})}{\mathrm{d}z} = \frac{3}{8}\,(1+z^2)\,\sigma^{\mathrm{SM}}_{q\bar{q}} + \frac{5}{8}\,(1-3z^2+4z^4)\,\sigma^G_{q\bar{q}} + \frac{5}{8}\,(1-z^4)\,\sigma^G_{gg}, \tag{28}$$

$$\frac{\mathrm{d}\sigma(V_{ll})}{\mathrm{d}z} = \frac{3}{8}\,(1+z^2)\,(\sigma^{\mathrm{SM}}_{q\bar{q}} + \sigma^V_{q\bar{q}}), \tag{29}$$

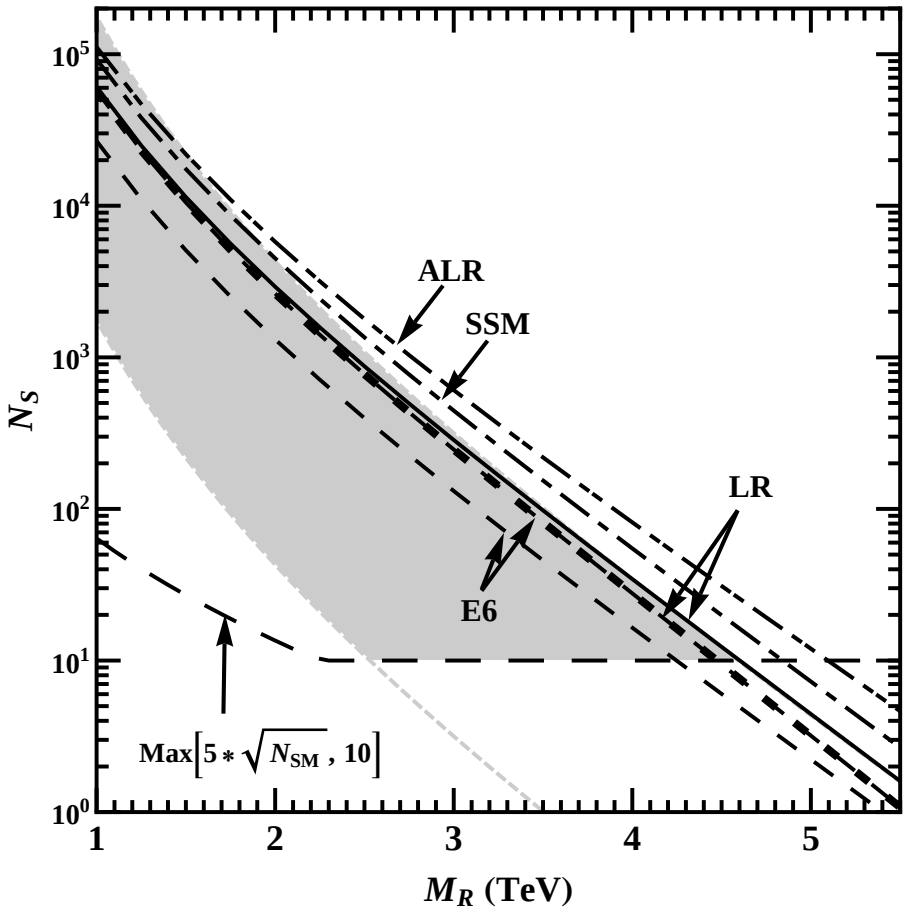

Figure 2: Same as in Fig. 1 but for number of resonance events N_S vs. M_R ($R = G, Z'$) for graviton and Z' resonant production and the minimum number of signal events needed to detect the resonances above the background in the process $pp \to l^+l^- + X$ ($l = e, \mu$). The shaded area is the overlap of graviton and sneutrino signature spaces for $0.01 < c < 0.1$, with $\mathcal{L}_{\rm int} = 100$ fb^{-1}.

$$\frac{{\rm d}\sigma(S_{ll})}{{\rm d}z} = \frac{3}{8}\,(1+z^2)\,\sigma^{\rm SM}_{q\bar{q}} + \frac{1}{2}\,\sigma^{S}_{q\bar{q}}. \tag{30}$$

Corresponding to Eqs. (28)–(30), the integrated pp production cross sections for the G, V and S hypotheses are given by

$$\sigma(G_{ll}) = \sigma^{\rm SM}_{q\bar{q}} + \sigma^{G}_{q\bar{q}} + \sigma^{G}_{gg}, \quad \sigma(V_{ll}) = \sigma^{\rm SM}_{q\bar{q}} + \sigma^{V}_{q\bar{q}}, \quad \sigma(S_{ll}) = \sigma^{\rm SM}_{q\bar{q}} + \sigma^{S}_{q\bar{q}}. \tag{31}$$

Detector cuts are not taken into account in the above Eqs. (28)–(31). We shall use these relations for illustration purposes, in order to better expose the most important features of the method we use. The final numerical results, as well as the relevant figures that will be presented in the sequel refer to the full calculation, with detector cuts taken into account. It turns out, however, that such results are numerically close to those derived from the application of Eqs. (28)–(31).

The angular distributions arising from the spin-2, spin-1 and spin-0 resonances are represented in Fig. 3, for the same peak masses M_R in the three hypotheses and the same number of signal events, N_S, under the peak.

To assess the identification power of the LHC of distinguishing the spin-2 RS resonance from both spin-1 and spin-0 exchanges, we adopt the integrated center-edge asymmetry $A_{\rm CE}$

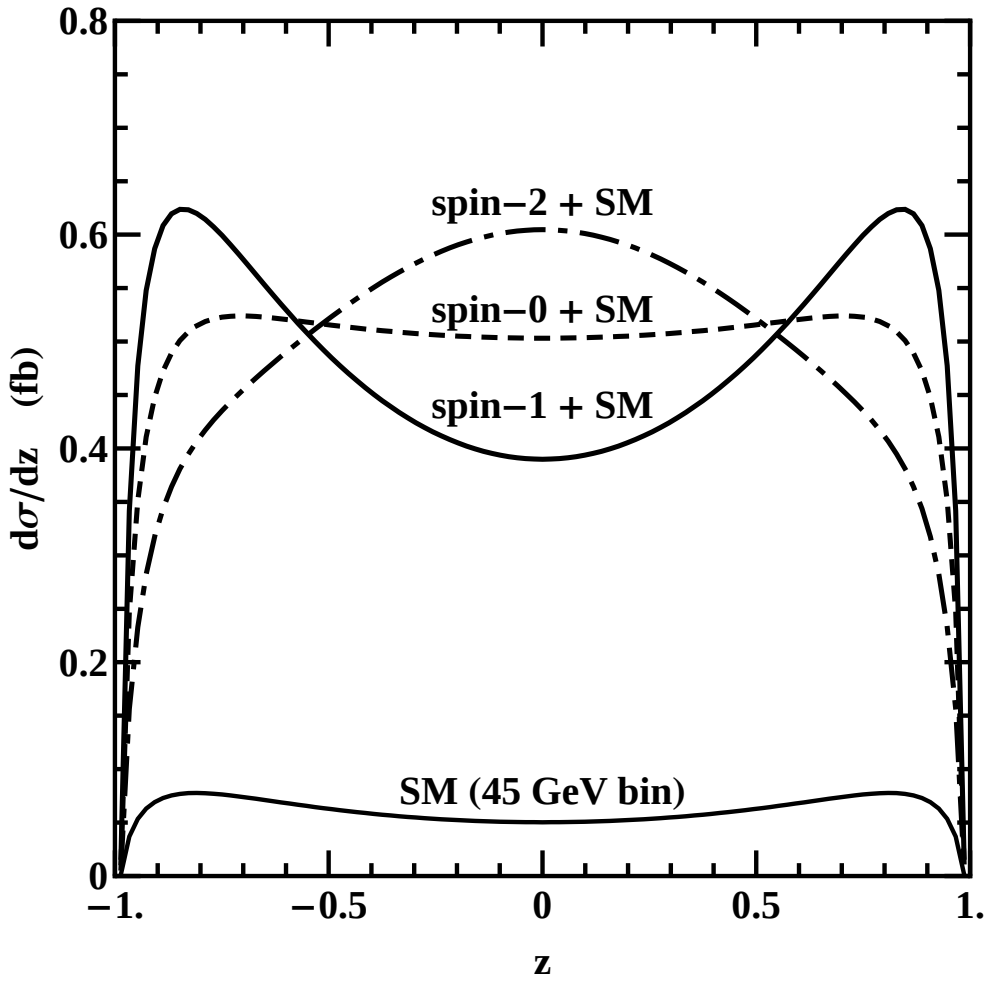

Figure 3: Angular distribution of leptons in the dilepton center of mass system for (i) spin-2 graviton resonant production, $\mathrm{d}\sigma(pp \to G \to l^+l^-)/\mathrm{d}z$, in the RS model with c=0.01; (ii) spin-0 resonant production, $\mathrm{d}\sigma(pp \to S \to l^+l^-)/\mathrm{d}z$; (iii) spin-1 resonant production, $\mathrm{d}\sigma(pp \to V \to l^+l^-)/\mathrm{d}z$. We take $M_R = 1.6$ TeV and assume equal numbers of resonant DY events.

introduced in Refs. [10, 11] and defined as:

$$A_{\mathrm{CE}}(M_R) = \frac{\sigma_{\mathrm{CE}}(R_{ll})}{\sigma(R_{ll})}, \tag{32}$$

with the "center minus edge" cross section:

$$\sigma_{\mathrm{CE}} \equiv \left[\int_{-z^*}^{z^*} - \left(\int_{-z_{\mathrm{cut}}}^{-z^*} + \int_{z^*}^{z_{\mathrm{cut}}}\right)\right] \frac{\mathrm{d}\sigma(R_{ll})}{\mathrm{d}z}\,\mathrm{d}z. \tag{33}$$

Here: $0 < z^* < z_{\mathrm{cut}}$ is a, a priori free, value of $\cos\theta_{\mathrm{cm}}$ that defines the separation between the "center" and the "edge" angular regions; in the approximation $z_{\mathrm{cut}} = 1$, $\mathrm{d}\sigma(R_{ll})/\mathrm{d}z$ are given by Eqs. (28)–(30) and the total cross sections $\sigma(R_{ll})$ by Eq. (31).

We assume that a deviation from the SM is discovered in the cross section for dilepton production at LHC in the form of a narrow peak in the dilepton invariant mass, and attempt the determination of the domain in the RS parameter space where such a peak can be *identified* as being caused by the spin-2 RS exchange, and the spin-0 and spin-1 hypotheses excluded. We also assume the integrated center-edge asymmetry evaluated within the RS model to be

consistent with the measured data, and call this spin-2 model the "true" or "best-fit"model. We want to assess the level at which this "true" model is distinguishable from the other hypotheses, with spin-0 and spin-1, that can compete with it as sources of a resonance peak in dilepton production yielding in particular the same number of signal events.

The explicit z^*-dependence of the center-edge asymmetries for the three cases of interest here, obtained from Eqs. (28)–(31) and Eqs. (32)–(33) are, in the same notations:

$$A^G_{\rm CE} = \epsilon^{\rm SM}_q\, A^V_{\rm CE} + \epsilon^G_q \left[2\, z^{*5} + \frac{5}{2}\, z^*(1 - z^{*2}) - 1\right] + \epsilon^G_g \left[\frac{1}{2}\, z^*(5 - z^{*4}) - 1\right], \tag{34}$$

$$A^V_{\rm CE} \equiv A^{\rm SM}_{\rm CE} = \frac{1}{2}\, z^*(z^{*2} + 3) - 1, \tag{35}$$

$$A^S_{\rm CE} = \epsilon^{\rm SM}_q\, A^V_{\rm CE} + \epsilon^S_q\, (2\, z^* - 1). \tag{36}$$

Here, ϵ^G_q, ϵ^G_gs and $\epsilon^{\rm SM}_q$ are the fractions of resonant events for $q\bar{q}, gg \to G \to l^+l^-$ and SM background, respectively, with $\epsilon^G_q + \epsilon^G_g + \epsilon^{\rm SM}_q = 1$. They are determined by the ratios of $\sigma^G_{q\bar{q}}$, etc., of Eq. (28) and $\sigma(G_{ll})$ of Eq. (31). Analogous definitions hold for the other cases.

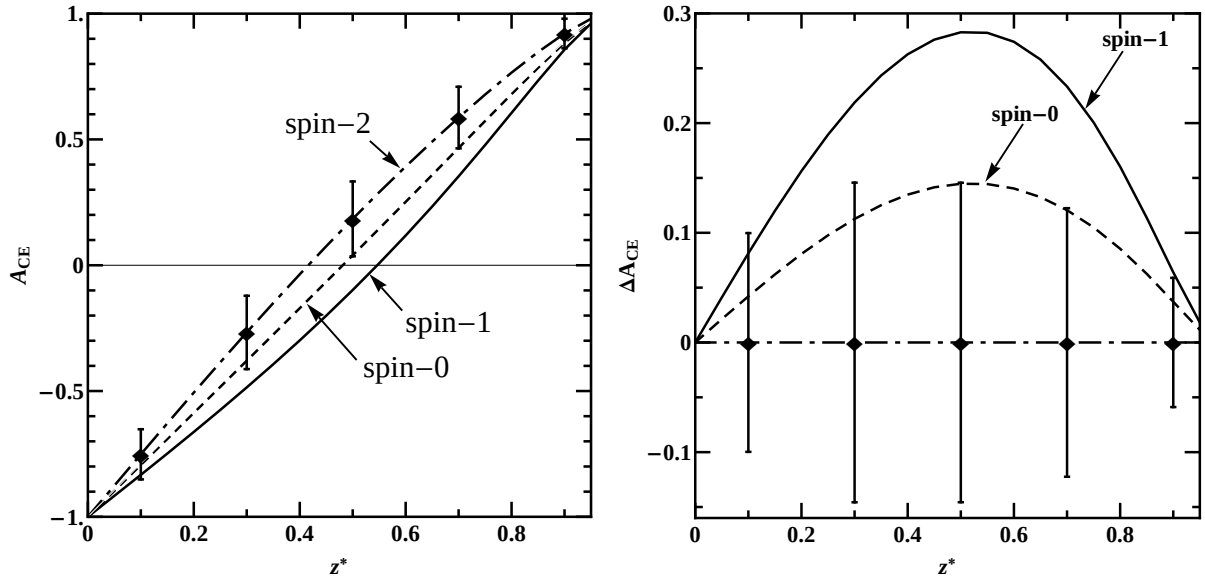

Figure 4: Left panel: $A_{\rm CE}$ *vs.* z^* for the spin-2 resonance G at c =0.01 and M_R=1.6 TeV (dot-dashed curve), and for the spin-0 (dashed curve) and spin-1 (solid curve) hypotheses, all for the same M_R and number of events. The error bar at $z^* = 0.5$ is within the identification reach on G (at the 2σ level) for $\mathcal{L}_{\rm int} = 100$ fb^{-1} as explained in the text. Right panel: Asymmetry deviations, $\Delta A_{\rm CE}$, of the spin-1 and spin-0 hypotheses from the RS one, compared with the uncertainties on $A^G_{\rm CE}$.

As an example, in Fig. 4 (left panel) the center-edge asymmetry $A_{\rm CE}$ is depicted as a function of z^* for resonances with different spins, same mass $M_R = 1.6$ TeV and same number N_S of signal events under the peak. The dot-dashed curve corresponds to the spin-2 RS graviton with $c = 0.01$. The calculation is performed using detector cuts as well as the SM background have been accounted for. Actually, the z^*-behavior of $A_{\rm CE}(z^*)$ resulting from the full calculation is found essentially equivalent to those presented in Eqs. (34)–(36). Differences are appreciable only for z^* close to 1, and turn out to have negligible impact on the numerical determinations of the identification reaches presented in the sequel, where the relevant chosen values of z^* are in a range around 0.5. Indeed, since numerically the χ^2 turns out to have a smooth dependence there, for definiteness we will present the results obtained from $A_{\rm CE}(z^* = 0.5)$.

The deviations of the $A_{\rm CE}$ asymmetry from the prediction of the RS model, caused by the spin-0 exchange

$$\Delta A_{\rm CE} = A^G_{\rm CE} - A^S_{\rm CE} \tag{37}$$

and that caused by the spin-1 exchange

$$\Delta A_{\rm CE} = A^G_{\rm CE} - A^V_{\rm CE}, \tag{38}$$

respectively, are depicted in Fig. 4 (right panel). The identification potential depends, of course, from the available statistics (as well as on systematic uncertainties). In the example of Fig. 4, the vertical bars attached to the dot-dashed curve represent the 2σ statistical uncertainty on the $A_{\rm CE}$ of the RS graviton model, assumed to be the "true" model consistent with the data as stated above, with the values of M_G and c reported in the caption and integrated LHC luminosity of 100 fb^{-1}. One reads from Fig. 4 that, at such (high) luminosity, the spin-2 RS graviton with mass $M_G = 1.6$ TeV and coupling $c = 0.01$ can, indeed, be discriminated from the other spin-hypotheses by means of $A_{\rm CE}$ at $z^* \simeq 0.5$.

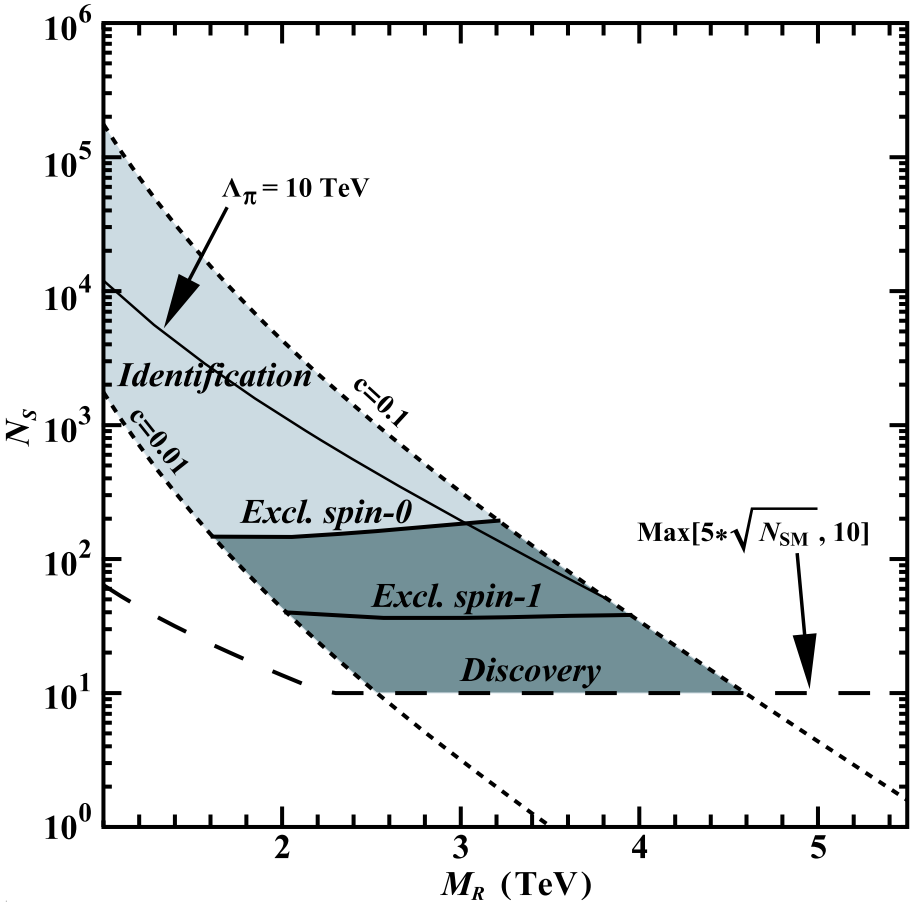

Figure 5: Same as in Fig. 1 but with exclusion limits and identification reach at 95% C.L. and $\mathcal{L}_{\rm int} = 100$ fb^{-1}. The channels $l = e, \mu$ are combined. The theoretically favored region, limited by the $\Lambda_\pi = 10$ TeV and $c = 0.1$ lines, is also indicated.

Actually, Eqs. (35) and (36) show the peculiar feature of $A_{\rm CE}(z^*)$, that for same number of signal events:

$$A^S_{\rm CE}(z^*) > A^V_{\rm CE}(z^*), \tag{39}$$

for all values of $0 < z^* < 1$. This property is of course reproduced in Fig. 4, and allows to conclude that, in order to identify the spin-2 graviton resonance, if one is able to exclude the spin-0 hypothesis, the whole class of spin-1 models will then automatically be excluded, so that

the spin-2 *identification* from the spin-1 hypothesis would be model-independent. Stated in a statistical language, Eq. (39) explicitly realizes the statement that discrimination of the spin-2 RS resonance from the spin-1 hypothesis requires, for a given confidence level, less events than the discrimination from the spin-0 one, as also noted in Ref. [6].

Equivalent to the above procedure, the identification M_G and c can be assessed by means of a "conventional" (and simple minded) χ^2 criterion, where the χ^2 function is defined as:

$$\chi^2 = \left[\frac{\Delta A_{\rm CE}}{\delta A_{\rm CE}}\right]^2, \tag{40}$$

with $\Delta A_{\rm CE}$ represented by Eqs. (37) and (38) to obtain the exclusion domains of the spin-0 and spin-1 hypotheses, respectively, and the statistical uncertainty

$$\delta A_{\rm CE} = \sqrt{\frac{1-\left(A_{\rm CE}^G\right)^2}{\epsilon_l \mathcal{L}_{\rm int}\sigma(G_{ll})}}. \tag{41}$$

Like before, the RS model can be assumed to be the "true" one, and the (95% C.L.) exclusion domains of spin-0 and spin-1 can be determined by requiring $\chi^2 = 3.84$. The derived results for N_S are displayed in Fig. 5 as a function of graviton mass M_G (95% C.L.). The resulting domain defines the identification reach on the spin-2 of the resonance.

Numerically, one can read from Fig. 5 that, for $\mathcal{L}_{\rm int} = 100$ fb^{-1} the spin-1 hypothesis may be excluded up to $M_G = 2.0$ TeV for $c = 0.01$ and $M_G = 4.0$ TeV for $c = 0.1$. The spin-2 of the RS resonance can be identified by spin-0 exclusion up to $M_G = 1.6$ TeV for $c = 0.01$ and $M_G = 3.2$ TeV for $c = 0.1$.

In conclusion, we have considered the RS scenario, assuming a discovery can be made in the form of a resonance in the dilepton cross section. We have determined by an $A_{\rm CE}$-based analysis up to what mass the spin-2 property can be established. This basically amounts to excluding the spin-0 hypothesis, in which case the spin-1 alternative will be automatically excluded. Additionally, we point out that in the parameter space where this spin determination is possible, the second resonance, with its characteristic mass, is also visible.

Acknowledgements
We would like to thank Prof. P. Osland and Prof. N. Paver for the enjoyable collaboration on the subject matter covered here.

References

[1] For details of the analysis and original references, see P. Osland, A. A. Pankov, N. Paver and A. V. Tsytrinov, Phys. Rev. D **78**, 035008 (2008) [arXiv:0805.2734 [hep-ph]].

[2] L. Randall and R. Sundrum, Phys. Rev. Lett. **83** (1999) 3370 [arXiv:hep-ph/9905221]; *ibid.* Phys. Rev. Lett. **83** (1999) 4690 [arXiv:hep-th/9906064].

[3] V. A. Rubakov, Phys. Usp. **44**, 871 (2001) [Usp. Fiz. Nauk **171**, 913 (2001)] [arXiv:hep-ph/0104152].

[4] B. C. Allanach, K. Odagiri, M. A. Parker and B. R. Webber, JHEP **0009**, 019 (2000) [arXiv:hep-ph/0006114].

[5] B. C. Allanach, K. Odagiri, M. J. Palmer, M. A. Parker, A. Sabetfakhri and B. R. Webber, JHEP **0212**, 039 (2002) [arXiv:hep-ph/0211205].

[6] R. Cousins, J. Mumford, J. Tucker and V. Valuev, JHEP **0511**, 046 (2005).

[7] I. Belotelov *et al.*, "Search for Randall-Sundrum graviton decay into muon pairs," CERN-CMS-NOTE-2006-104.

[8] D. Feldman, Z. Liu and P. Nath, JHEP **0611**, 007 (2006) [arXiv:hep-ph/0606294].

[9] A. Abulencia *et al.* [CDF Collaboration], Phys. Rev. Lett. **95**, 252001 (2005) [arXiv:hep-ex/0507104].

[10] E. W. Dvergsnes, P. Osland, A. A. Pankov and N. Paver, Phys. Rev. D **69**, 115001 (2004) [arXiv:hep-ph/0401199].

[11] P. Osland, A. A. Pankov and N. Paver, Phys. Rev. D **68**, 015007 (2003) [arXiv:hep-ph/0304123].

[12] J. Kalinowski, R. Ruckl, H. Spiesberger and P. M. Zerwas, Phys. Lett. B **406** (1997) 314 [arXiv:hep-ph/9703436]; *ibid.* Phys. Lett. B **414** (1997) 297 [arXiv:hep-ph/9708272];
T. G. Rizzo, Phys. Rev. D **59** (1999) 113004 [arXiv:hep-ph/9811440];
R. Barbier *et al.*, Phys. Rept. **420**, 1 (2005) [arXiv:hep-ph/0406039].

[13] B. Allanach *et al.* [R parity Working Group Collaboration], arXiv:hep-ph/9906224.

[14] For reviews see, *e.g.*: J. L. Hewett and T. G. Rizzo, Phys. Rept. **183** (1989) 193;
A. Leike, Phys. Rept. **317** (1999) 143 [arXiv:hep-ph/9805494];
P. Langacker, arXiv:0801.1345 [hep-ph].

[15] H. Davoudiasl, J. L. Hewett and T. G. Rizzo, Phys. Rev. Lett. **84** (2000) 2080 [arXiv:hep-ph/9909255]; *ibid.* Phys. Rev. D **63** (2001) 075004 [arXiv:hep-ph/0006041].

[16] V. M. Abazov *et al.* [D0 Collaboration], Phys. Rev. Lett. **100**, 091802 (2008) [arXiv:0710.3338 [hep-ex]].

[17] M. S. Carena, A. Daleo, B. A. Dobrescu and T. M. P. Tait, Phys. Rev. D **70**, 093009 (2004) [arXiv:hep-ph/0408098].

[18] T. Han, J. D. Lykken and R. J. Zhang, Phys. Rev. D **59**, 105006 (1999) [arXiv:hep-ph/9811350].

[19] G. F. Giudice, R. Rattazzi and J. D. Wells, Nucl. Phys. B **544**, 3 (1999) [arXiv:hep-ph/9811291].

[20] J. Bijnens, P. Eerola, M. Maul, A. Mansson and T. Sjostrand, Phys. Lett. B **503**, 341 (2001) [arXiv:hep-ph/0101316].

[21] "ATLAS: Detector and physics performance technical design report. Volume 1," CERN-LHCC-99-14
"ATLAS detector and physics performance. Technical design report. Vol. 2," CERN-LHCC-99-15

[22] CMS Collaboration, "The CMS Physics Technical Design Report, Volume 1," CERN/LHCC 2006-001 (2006). CMS TDR 8.1
CMS Collaboration, "The CMS Physics Technical Design Report, Volume 2," CERN/LHCC 2006-021 (2006). CMS TDR 8.2

[23] J. Pumplin, D. R. Stump, J. Huston, H. L. Lai, P. Nadolsky and W. K. Tung, JHEP **0207**, 012 (2002) [arXiv:hep-ph/0201195].